Molecular Phylogenetics and Evolution 185 (2023) 107829

Contents lists available at ScienceDirect

Molecular Phylogenetics and Evolution

journal homepage: www.elsevier.com/locate/ympev

Ocean crossers: A tale of disjunctions and speciation in the dwarf-fruticose *Lichina* (lichenized *Ascomycota*)

Isaac Garrido-Benavent [a,b,*], Asunción de los Ríos [c], Jano Núñez-Zapata [b], Rüdiger Ortiz-Álvarez [d], Matthias Schultz [e], Sergio Pérez-Ortega [b]

[a] Departament de Botànica i Geologia, Facultat de Ciències Biològiques, Universitat de València, C/ Doctor Moliner 50, E-46100 Burjassot, València, Spain
[b] Department of Mycology, Real Jardín Botánico (CSIC), Plaza Murillo 2, E-28014 Madrid, Spain
[c] Department of Biogeochemistry and Microbial Ecology, National Museum of Natural Sciences (MNCN-CSIC), Serrano 115 dpdo, E-28045 Madrid, Spain
[d] Department of International Science, Spanish Federation of Science and Technology (FECYT), C/ Pintor Murillo 15, E-28100 Alcobendas, Madrid, Spain
[e] Herbarium Hamburgense, Institute of Plant Science and Microbiology, University of Hamburg, Ohnhorststrasse 18, D-22609 Hamburg, Germany

ARTICLE INFO

Keywords:
Biogeography
Dispersal
Evolution
Integrative taxonomy
Lichen
Lichenized fungi
Lichinomycetes
Phylogeography
Population genetics
Subantarctic

ABSTRACT

Lichens thrive in rocky coastal areas in temperate and cold regions of both hemispheres. Species of the genus *Lichina*, which form characteristic black fruiting thalli associated with cyanobacteria, often create distinguishable bands in the intertidal and supralittoral zones. The present study uses a comprehensive specimen dataset and four gene loci to (1) delineate and discuss species boundaries in this genus, (2) assess evolutionary relationships among species, and (3) infer the most likely causes of their current geographic distribution in the Northern and Southern hemispheres. A dated phylogeny describes the time frame in which extant disjunctions of species and populations were established. The results showed that the genus is integrated by four species, with *Lichina pygmaea*, *L. confinis* and the newly described *L. canariensis* from rocky seashores in the Canary Islands, occurring in the Northern Hemisphere, whereas *L. intermedia* is restricted to the Southern Hemisphere. *Lichina intermedia* hosted a much higher intraspecific genetic diversity than the other species, with subclades interpreted as species-level lineages by the different species delimitation approaches. However, a conservative taxonomic approach was adopted. This species showed a striking disjunct distribution between Australasia and southern South America. The timing for the observed interspecific and intraspecific divergences and population disjunctions postdated continental plate movements, suggesting that long-distance dispersal across body waters in the two hemispheres played a major role in shaping the current species distributions. Such ocean crossings were, as in *L. canariensis*, followed by speciation. New substitution rates for the nrITS of the genus *Lichina* were inferred using a tree spanning the major *Ascomycota* lineages calibrated using fossils. In conclusion, this work lays the foundation for a better understanding of the evolution through time and space of maritime lichens.

1. Introduction

For the naturalist, the rocky coasts of most of the planet's oceans are a paradigm of diversity of green, brown, and red macroalgae. These organisms constitute the main primary producers in these habitats, reaching high biomass levels, despite a life under harsh abiotic conditions. Although much less conspicuous, fungi also thrive in these habitats. Most of them are endophyte microfungi sheltered on macroalgae thalli (Godinho et al. 2013; Flewelling et al. 2015), which show biotechnological activities such as the carrageenolytic and agarolytic (Furbino et al. 2018). Other fungi, mostly ascomycetes, are known to form various symbiotic associations with these algae. For example, the dothideomycete *Stigmidium ascophylli* (Cotton) Aptroot associates with the well-known Atlantic brown alga *Ascophyllum nodosum* (L.) Le Jolis; the eurotiomycete *Mastodia* spp. interacts with several species of the green alga *Prasiola* at a bipolar scale (Kohlmeyer et al. 2004; Garrido-Benavent et al. 2018), or also the eurotiomycete *Turgidosculum ulvae* (M. Reed) Kohlm. & E. Kohlm. associates with the green alga *Blidingia minima* (Nägeli ex Kützing) Kylin along the west coast of North America (Pérez-Ortega et al., 2018). In addition, species of the genus

* Corresponding author.
E-mail addresses: Isaac.Garrido@uv.es (I. Garrido-Benavent), arios@mncn.csic.es (A. de los Ríos), janoalexnz@gmail.com (J. Núñez-Zapata), rudigerortiz@gmail.com (R. Ortiz-Álvarez), matthias.schultz@uni-hamburg.de (M. Schultz), sperezortega@rjb.csic.es (S. Pérez-Ortega).

https://doi.org/10.1016/j.ympev.2023.107829
Received 15 July 2022; Received in revised form 24 December 2022; Accepted 26 May 2023
Available online 27 May 2023

Collemopsidium (Dothideomyceta) associate with the brown alga *Pelvetia canaliculata* (L.) Decaisne & Thuret (Kohlmeyer et al. 2004; Pérez-Ortega et al. 2016).

Typical lichen associations, which have been recently re-defined by Hawksworth and Grube (2020) as "self-sustaining ecosystems formed by the interaction of an exhabitant fungus and an extracellular arrangement of one or more photosynthetic partners and an indeterminate number of other microscopic organisms", also occur in rocky coasts of temperate to high latitudes in both hemispheres forming, in some cases, distinctive band-like zones (Lamb 1948; Brodo and Santesson 1997; Orange 2012; Pérez-Ortega et al. 2016). Such common arrangement in horizontal bands is also observed in macroalgae and probably stems from the different tolerance of diverse species to sudden changes in moistening, solar radiation, temperature, and salinity (Chappuis et al. 2014; Delmail et al. 2013). Although a high diversity of lichen forming fungi can thrive in maritime habitats (Fletcher 1980), the supralittoral and intertidal zones are dominated almost exclusively by the *Verrucariaceae*, *Xanthopyreniaceae* and *Lichinaceae* families.

Species of the ascomycete genus *Lichina* C. Agardh, the type genus of the family *Lichinaceae*, often form distinctive black bands in the intertidal and supralittoral zones. *Lichina* species are characterized by their dwarf-fruticose thalli and their symbiotic association with cyanobacteria. The knowledge on the biology of this cyanolichen genus has gained impetus in the last years due to the comprehensive reviews about mycobiont-cyanobiont interactions (Ortiz-Álvarez et al. 2015), taxonomy (Schultz 2017), and the diversity of associated bacteria (West et al. 2018) and photobionts (Chrismas et al. 2021). In the first work, different genetic lineages of the cyanobacteria *Rivularia* were found in association with *Lichina pygmaea* (Lightf.) C. Agardh and *L. confinis* (O.F. Müll) C. Agardh, two species widespread in the Northeast Atlantic that grow on the same rocky shores but occupying different littoral zones. The former species appears in the upper intertidal zone, and therefore it becomes submerged periodically, and the latter grows in the supralittoral, which is only directly affected by sea spray. It was suggested that the association to different lineages of *Rivularia*, which had an evolutionary origin preceding that of *Lichina* mycobionts, had driven ecological speciation in these two species. Furthermore, Ortiz-Álvarez et al. (2015) revealed the existence of an undescribed species restricted to the Canary Islands and phylogenetically close to *L. pygmaea*, which was tentatively named "*L. canariensis*". Later, Schultz (2017) used molecular sequence and morphological data to support the distinction of New Zealand maritime specimens resembling *L. pygmaea* as a different species, *L. intermedia* (C. Bab.) M. Schultz. Our recent discovery of populations of a puzzling species of *Lichina* on the coast of Chile raised the question of whether these specimens might belong to the New Zealand species *L. intermedia*. Thus, despite such recent advances in the biology of *Lichina*, several questions concerning the fungal partner of the symbiosis remain open: (1) Which are the phylogenetic relationships among the four aforementioned maritime species of *Lichina*, including the undescribed "*L. canariensis*"?; (2) Do specimens from yet unexplored areas, such as the rocky shores in southern South America, constitute a new taxon and, if so, where are they placed phylogenetically?; (3) How are the different *Lichina* species structured genetically at the geographic scale?; and (4) When do these species diverged and diversified, and which is the most probable temporal window in which their current geographic distribution originated?

The present study combines analytical approaches at intra- and interspecific levels to answer these questions, taking advantage of an extended specimen dataset with newly collected specimens worldwide, merged with those published previously in Ortiz-Álvarez et al. (2015) and Schultz (2017). Compared to these two works, the molecular sequence dataset is expanded to include four loci. Finally, at the taxonomic level, the species from the Canary Islands "*L. canariensis*" is here formally described after the high support found in the species delimitation analyses. The present phylogeographic study provides new insights into the evolutionary history of this genus of cyanolichens occurring in maritime habitats.

2. Materials and methods

2.1. Taxon sampling and morphological studies

This study used a collection of 109 specimens of *Lichina* spp. assembled by the authors (Supplementary Table S1), deposited in the herbarium of the Real Jardín Botánico of Madrid (MA), Spain. Geographically, sampling covered most of the known extant worldwide distribution of *Lichina* spp. and included the Macaronesian archipelagos (Canary and Azores islands), the Iberian Peninsula, France, the British Isles and Iceland in the Northern Hemisphere, and Chile, New Zealand and Tasmania in the Southern Hemisphere. For the molecular study described below, DNA sequences generated by Schultz (2017) from specimens collected in Germany, Russia, Sweden, Portugal and New Zealand (including the Chatham Islands) were also considered. *Psoroticchia lutophila* Arnold, *Peltula* sp. and *Lichinella* sp. were used as outgroup to root phylogenetic trees. Author citations follow MycoBank (https://www.mycobank.org/) or Index Fungorum (https://www.indexfungorum.org/).

Specimens were examined under a Leica S8APO dissecting stereomicroscope, and macroscopic photographs were taken with a Leica EC3 image capture system. Hand-cut sections of ascomata were observed using a Zeiss Axioplan 2 microscope fitted with 'Nomarski' differential interference contrast (DIC) and a Zeiss AxioCam digital camera was used to take photographs. Microscopic observations and measurements were made on material mounted in water by means of the Zeiss Axiovision 4.8 image analyser system. Lactophenol blue was used for examination of fertile and vegetative hyphae. Measurements are given as the average, maximum and minimum values discarding the 10% highest and lowest values (the former two in parentheses).

2.2. Laboratory procedures and DNA sequence edition

An apical branch fragment of each specimen was placed in 1.5 mL Eppendorf tube, frozen at −80 °C and then pulverized with metal beads using a TissueLyserII (Retsch). The DNA was extracted using the E.Z.N.A.® Forensic DNA kit (Omega Bio-Tek) following the manufacturers' instructions (standard protocol). Four putatively unlinked nuclear fungal markers were targeted: the Internal Transcribed Spacer of the ribosomal DNA (nrITS), the small subunit of the mitochondrial ribosomal RNA gene (mtSSU), the second largest subunit of the RNA polymerase II gene (RPB2), and the hypothetical protein *LNS2* (Stielow et al. 2015). For the dating analyses, four additional markers were amplified from a selected number of specimens of each *Lichina* species and the outgroup: the nuclear ribosomal small (nuSSU) and large (nuLSU) subunits, the largest subunit of the RNA polymerase II (RPB1), and the translation elongation factor 1-α (TEF1α). Primer pairs, including newly designed RPB1/2 and TEF1α, are available in Supplementary Table S2. PCR reactions were performed in a total volume of 15 µl, containing 2 µl of template DNA, 0.5 µl of each primer (10 µM), 6.5 µl of MyTaq Mix (MyTaq DNA Polymerase [Bioline] and dNTPs); distilled water was added to reach the final volume. PCR reactions were done in an Eppendorf Mastercycle EP gradient S thermal cycler, and amplification conditions are summarized in Supplementary Table S3. PCR products were purified using ExoSAP-IT™ PCR Product Cleanup Reagent (ThermoFisher) according to manufacturer instructions, and sequenced by Macrogen Inc. (Madrid, Spain) using the same primer set as for PCR amplification. Sequence contigs were assembled using SeqMan v.5.07© (Lasergene, DNA Star Inc., WI, USA). Sequences showing ambiguous sites were visually corrected and collapsed into locally co-occurring haplotypes to avoid artificial inflation of genetic variability. Geneious® v.9.0.2 was used to annotate introns and exons in protein-coding markers (*LNS2*, RPB1/2, and TEF1α).

2.3. Single-locus alignments and phylogenetic relationships

Sequence alignments were carried out independently for nrITS, mtSSU, RPB2 and *LNS2* with MAFFT v.7.308 (Katoh and Standley 2013) as implemented in Geneious v.9.0.2. The base nrITS and mtSSU sequence datasets contained the newly obtained sequences as well as those published previously in Schultz (2017). Due to unsolvable issues at the PCR amplification step, different outgroup taxa were used for each single-locus alignment: the species *Psorotichia lutophila* was used for nrITS and mtSSU alignments; *Peltula* sp. for RPB2; and *Peltula* sp. and *Lichinella* sp. for *LNS2*. The specified alignment parameters were the following: the FFT-NS-I × 1000 algorithm, the 200 PAM / k = 2 scoring matrix, a gap open penalty of 1.5, and an offset value of 0.123. The resulting nrITS alignment was manually optimized to trim ends of longer sequences that included part of the 18S-28S ribosomal subunits, and to replace gaps at the ends of shorter sequences with an IUPAC base representing any base ("N"). Large introns found only in the outgroup in the nrITS, mtSSU, and RPB2 alignments were also manually deleted. The final version of each alignment was submitted to the software DnaSP v.5.10 (Librado and Rozas 2009) to compute various statistics of DNA polymorphism: haplotype diversity (*Hd*) excluding sites with gaps or missing data, the average number of nucleotide differences (*k*), the nucleotide diversity (π) with and without using the Jukes and Cantor correction, and the number of segregating sites (*S*), parsimony informative sites and haplotypes (*h*).

The online version of RAxML-HPC2 hosted at the CIPRES Science Gateway (Stamatakis 2006; Stamatakis et al. 2008; Miller et al. 2010) was chosen to estimate a Maximum Likelihood (ML) phylogeny for the four marker dataset. The nrITS was partitioned into ITS1 + 2 and 5.8S, whereas the two-protein coding RPB2 and *LNS2* were partitioned by codon position. The GTRGAMMA nucleotide substitution model was chosen for all partitions. One thousand rapid bootstrap pseudoreplicates were conducted to evaluate nodal support. The resulting trees were drawn with the iTOL web tool (Letunic and Bork 2021), and Adobe Illustrator CS5 was used for artwork. Tree nodes with bootstrap support (BS) values equal or higher than 70% were regarded as significantly supported.

2.4. Haplotype networks and species genetic stratification

Relationships among haplotypes were inferred under a statistical parsimony network in PopART v.1.7 (Leigh and Bryant 2015) using the method TCS (Templeton et al. 1992). Previously, haplotypes for each marker were collapsed using DnaSP v.5.10, including gaps and invariable sites. For the nrITS dataset, a second version of the alignment was built after removing ambiguously aligned regions and large gaps automatically with Gblocks v.0.91b (Castresana 2000), using the less stringent parameter settings. Furthermore, BAPS v.6 (Corander and Marttinen 2006; Corander et al. 2008) was used to quantify genetic stratification in multi-locus genotype data in *Lichina* spp. under an admixture model. Sequence data for those specimens with available full sequences for all four markers (66) was used after their transformation into single nucleotide polymorphism (SNP) files in MESQUITE v.3.01 (Maddison and Maddison 2014). Further parameter settings in the BAPS analysis can be found in Garrido-Benavent et al. (2018).

2.5. Species discovery and validation approach

To evaluate whether the phylogenetic structure revealed in the four single-locus topologies supported the existence of undescribed species in *Lichina* a species discovery-validation strategy was employed considering single- and multi-locus datasets. To build hypotheses of species limits in this genus (hereafter referred as to Models) nrITS data were considered, since this marker performs well as DNA barcode in most groups of fungi (Schoch et al. 2012). The Automatic Barcode Gap Discovery model (ABGD, Puillandre et al. 2012) was used to infer one-sided confidence limits for intra- and interspecific divergence based on the distribution of all pairwise distances. The nrITS alignment was built again, considering only unique sequences (43 haplotypes) and excluding the outgroup taxa. This dataset was submitted to ABGD (https://wwwabi.snv.jussieu.fr/public/abgd/abgdweb.html), setting the *Pmax* value to 0.01 (Puillandre et al. 2012), the model for genetic distance calculation to K2P, the transition/transversion ratio (TS/TV) calculated in MEGA-X (Kumar et al. 2018) using the T92 + Γ substitution model to 1.87, and the remaining model parameters to default. To assess whether species limits were consistently inferred across different parameter settings, the relative gap width (*X*) was set to varying levels: 0.5, 1, and 1.5. Models of species limits in *Lichina* also relied on results of the Poisson Tree Process (bPTP) model (Zhang et al. 2013), which was run at https://species.h-its.org/ptp using the rooted nrITS phylogenetic tree inferred above under a Maximum likelihood framework. In the bPTP run, the number of MCMC generations was set to 5×10^5, thinning to 500, the burn-in to 25%, and the outgroup was excluded.

A total of four models were defined, evaluated, and compared using the Bayes Factor Delimitation (BFD) method of Grummer et al. (2014), which allows for topological uncertainty in gene trees and incongruences among gene trees. This approach is preferred in scenarios of recent divergences or phylogeographic studies (e.g., Garrido-Benavent et al. 2018). A concatenated four locus dataset was constructed considering only the *Lichina* specimens for which the four markers were successfully sequenced (66). After removing specimens with identical sequences to avoid redundancies, the number of specimens left was 53, including the outgroup *Peltula* sp. *BEAST (Heled and Drummond 2010; Drummond et al. 2012) was used to build the four competing models. Parameter settings considered the following substitution models and partition schemes, as suggested by PartitionFinder v.1.1.1 (Lanfear et al. 2012): TrN + Γ (nrITS), HKY + I + Γ (mtSSU, *LNS2*-codon2, RPB2-codon2), HKY (*LNS2*-codon1, RPB2-codon1), and GTR + Γ (*LNS2*-codon3, RPB2-codon3). A birth–death process tree prior was imposed, and an uncorrelated relaxed lognormal molecular clock was chosen for the four markers, fixing the mean clock rate to 1.0 for nrITS whereas rates were co-estimated for the remaining markers under a uniform prior (1×10^{-5}, 6). Remaining analysis parameters were set as in Mitchell et al. (2021). Ten replicate *BEAST runs of 2×10^8 generations were conducted for each model, saving every 20000th tree, using the CIPRES Science Gateway. Tracer v.1.7 (Rambaut et al. 2018) was used to check for convergence, assuming effective sample sizes (ESS) above 200. The initial lack of convergence was solved by avoiding overparameterization, and therefore the HKY substitution model for the partition including the *LNS2*-codon3 and RPB2-codon3 was selected instead of GTR. Then, Bayes factors comparisons of Maximum Likelihood Estimates (MLE) for the four species boundary models were calculated using Path Sampling and Stepping-Stone (Lartillot and Philippe 2006; Xie et al. 2011), with default settings. 2lnBF > 10 indicates robust evidence against a model as compared with the best (Kass and Raftery 1995).

2.6. Estimating a time frame for speciation events in Lichina

Speciation events in the genus *Lichina* were time-framed using two alternative strategies. First, the inferred time tree published in the Mitchell et al. (2021) study was considered. It was based on a calibration approach that used six fossils and a dataset of six loci comprising members of all major ascomycete lineages (169 specimens in total), including data of nine *Lichina* specimens representing all known species, as well as the outgroup *Lichinella* sp. and *Peltula* sp. Further details on analyses, specimens' data table, and chronogram representation, are available in the above-mentioned work. Secondly, two different nrITS average mutation rates were imposed on the nrITS haplotype dataset, which comprised the different *Lichina* haplotypes and the outgroup *Psorotichia lutophila*. These rates were 2.52×10^{-3} substitutions per site per million years (*Erysiphales* in *Eurotiomycetes*, Takamatsu and Matsuda

2004) and 3.41 × 10^{-3} substitutions per site per million years (*Melanohalea* in *Lecanoromycetes*, Leavitt et al. 2012); the different rates are expected to accommodate the likely variability in substitution rates within family *Lichinaceae*. Analyses were conducted in BEAST v.1.8.1 (Drummond et al. 2012) and after Bayes Factors comparisons of different clock and tree models, runs implemented an uncorrelated lognormal relaxed molecular clock along a birth–death process tree prior, the TrN + Γ substitution model for the combined nrITS1 + nrITS2 partitions and the K80 + I for the 5.8S partition. Running conditions considered a chain length of 5 × 10^7 steps, saving 10^4 trees. The same analyses were implemented on a Gblocks-processed nrITS dataset to evaluate the influence of alignment uncertainty in dating results; for this dataset, nucleotide substitution models were GTR + Γ (nrITS1 + nrITS2) and JC + I (5.8S). In all analyses, an adequate burn-in was subsequently selected and convergence was checked in Tracer v.1.5 (available at: https://tree.bio.ed.ac.uk/software/tracer/). Then, the median heights of the post-burn-in tree samples, and the highest and lowest 95% highest posterior density values were annotated in TreeAnnotator v.1.8.1 (Drummond et al. 2012). FigTree v.1.4.0 (available at: https://tree.bio.ed.ac.uk/software/figtree/) was used to visualize 50% majority rule consensus trees.

2.7. Inference of a Lichina-specific nrITS substitution rate

Because different treatments of ambiguously aligned regions in highly variable markers, such as the nrITS, may cause an impact on dating results (Lücking 2019), the two aforementioned versions of the nrITS haplotype dataset were considered for calculating a specific nrITS substitution rate based on the time estimates generated in the fossil-calibrated chronogram. In particular, the time estimate for the node representing the divergence between the *L. pygmaea/L. canariensis* and the *L. confinis/L. intermedia* clades was imposed on the nrITS haplotype dataset using a normal prior with a mean value of 22.8 million years ago (hereafter referred as to Mya) and a standard deviation value of 4.75 Mya. To estimate the nrITS *ucld.mean* parameter in BEAST, a uniform prior with an initial value of 0.001, a lower value of 1 × 10^{-5}, and an upper value of 0.05 was given. Nucleotide substitution, clock and tree models were set as in the previous BEAST analyses, and the chain length was increased to 7.5 × 10^7 steps, although 10^4 trees were also saved. The mean heights of the post-burn-in tree samples, as well as the highest and lowest 95% highest posterior density values were annotated in TreeAnnotator v.1.8.1. The mean, median and highest and lowest values of the 95% highest posterior density interval for the node comprising all *Lichina* specimens were drawn from a time tree depicted in FigTree v.1.4.0.

3. Results

3.1. Molecular sequence data

The assembled dataset comprised 371 newly generated sequences: 94 nrITS (ingroup specimens: 92; outgroup: 2), 83 mtSSU, 93 partial RPB2, and 101 *LNS2* (ingroup: 99; outgroup: 2). GenBank accession numbers are in Supplementary Table S1 and alignments were deposited in FigShare (https://doi.org/10.6084/m9.figshare.21762803). The remaining outgroup mtSSU and RPB2 sequences, as well as the ingroup and outgroup nuSSU, nuLSU, RPB1 and TEF1α sequences were already published in Mitchell et al. (2021). The locus with the highest nucleotide diversity (π), the highest number of haplotypes (h), polymorphic sites (S), and parsimony-informative sites was the nrITS (Supplementary Table S4). It was followed by RPB2, which was the marker with the highest haplotype diversity (*Hd*). The shortest alignment was generated for the protein-coding marker *LNS2*; however, it showed higher levels of DNA polymorphism than the more commonly used mtSSU.

3.2. Molecular phylogenies and species delimitation

The ML analyses in RAxML generated single-locus phylogenies with lnL = -2485.5696 (nrITS), −1317.2424 (mtSSU), −2359.2153 (RPB2), and −827.7862 (*LNS2*). The inferred topologies are depicted in Fig. 1A. The nrITS tree showed two well-supported clades: one included *Lichina pygmaea* and the new species described below (see Taxonomy subsection), with a support of BS = 99%; the other revealed *L. confinis* as sister species of *L. intermedia*, with a BS = 84%. Clades representing individual species had BS values above 87%. The close relationship between *L. pygmaea* and *L. canariensis* was also well-supported in the mtSSU and RPB2 phylogenies, but not in the *LNS2* one. The chronogram inferred in the dating analysis using a six-locus dataset also corroborated the sister relationship between the pairs *L. pygmaea-L.canariensis* and *L. confinis-L. intermedia* (data not shown). *Lichina intermedia* always showed the highest intraspecific diversity, hosting a comparatively high number of subclades; however, there was not a clear segregation of clades according to geography. For example, the nrITS, mtSSU and *LNS2* topologies showed some specimens from Huinay (Chile) that were interspersed between New Zealand specimens.

The ABGD analyses revealed a clear barcode gap between *P* distance values ranging from 0.07 to 0.13 and across different values of *X*, suggesting four or five partitions (putative species) in the nrITS dataset. These partitions were consistent with a delimitation based on supported phylogenetic clades in the four-locus phylogeny (Fig. 1B). In contrast, the number of candidate species suggested by the bPTP method was 10 (Fig. 1B). Three of them were consistent with the ABGD delimitation and phylogenetic clades, and separated *L. pygmaea*, *L. confinis,* and the new *L. canariensis*; the remaining seven were allocated within *L. intermedia*, suggesting that even minor and unsupported clades in the four-locus phylogeny might be candidate species. Moreover, the optimal number of multi-locus mixture clusters inferred with BAPS was five (Fig. 2B). *Lichina confinis*, *L. pygmaea* and the new species were recovered in one cluster each, whereas *L. intermedia* encompassed two clusters: one being predominant and geographically widespread in the studied Southern Hemisphere range, and the other comprising a few individuals from New Zealand and Huinay. No signs of admixture were revealed by the BAPS analysis.

The four models evaluated and compared with BFD are summarized in Table 1. The best scoring model differed depending on the method used to sample the marginal likelihood, according to Bayes factor comparisons. In Path Sampling (PS), the best model was the one suggested by bPTP that considered 10 candidate species, closely followed by Model 3, which proposed five species, i.e., it divided the Southern Hemisphere *L. intermedia* into two candidate species, one restricted to southern South America, and the second distributed in Tasmania, New Zealand and the Chatham Islands. In Stepping-Stone (SS), the preferred model was the one considering five species based on the five-partition solution rendered by ABGD, and also by the multi-locus BAPS analysis. The second-best model was again Model 3. In both PS and SS, the worst model was the most conservative one (Model 1, four species), which is the more coherent with a delimitation based on the main phylogenetic clades shown in the four-locus phylogeny. Boxplots of the Maximum Likelihood Estimates (MLEs) obtained after running each model ten times showed a considerable overlap among the four models (Fig. 1B). Altogether, these results support the new species of *Lichina,* and therefore it is described in the following subsection.

3.3. Taxonomy

Lichina canariensis Pérez-Ort., de los Ríos & Garrido-Benavent.

MycoBank number: MB 843726.

Diagnosis: *Lichina canariensis* resembles *L. pygmaea*, from which it differs in having smaller stems and narrower branches.

Type: Spain, Las Palmas, Las Palmas de Gran Canaria, intertidal zone in Playa de las Canteras, 28°8′55″N; 15°25′59.5″W, 0 m asl, on volcanic

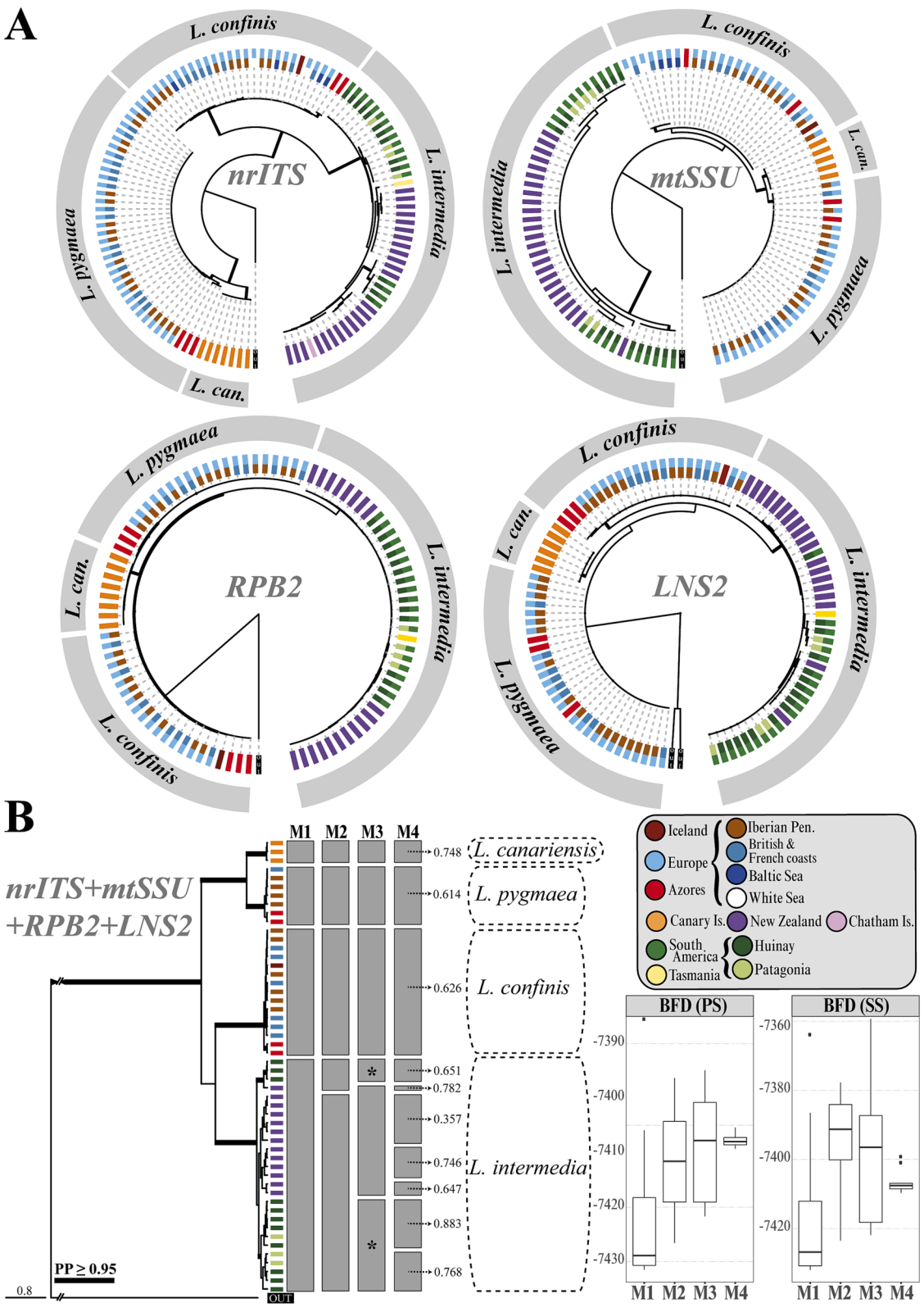

Fig. 1. Single- (A) and four-locus (B) phylograms showing the phylogenetic relationships among the four *Lichina* species; coloured bars at tips indicate the geographic origin (see legend below) of each collection; the black bar indicates the position of the outgroup; bold branches denote high nodal support in the single- (RAxML bootstrap values ≥ 70%) and four-locus (PP ≥ 0.95). In B, on the right margin of the phylogram, species delimitation models (M1 to M4) are represented, and their descriptions and motivations are shown in Table 1; values associated to the M4 column are Bayesian support values to delimited species in the bPTP analysis; boxplots represent Maximum Likelihood Estimates obtained after running each model ten times under the Path Sampling (PS, left) and Stepping-Stone (SS, right) algorithms to sample marginal likelihood.

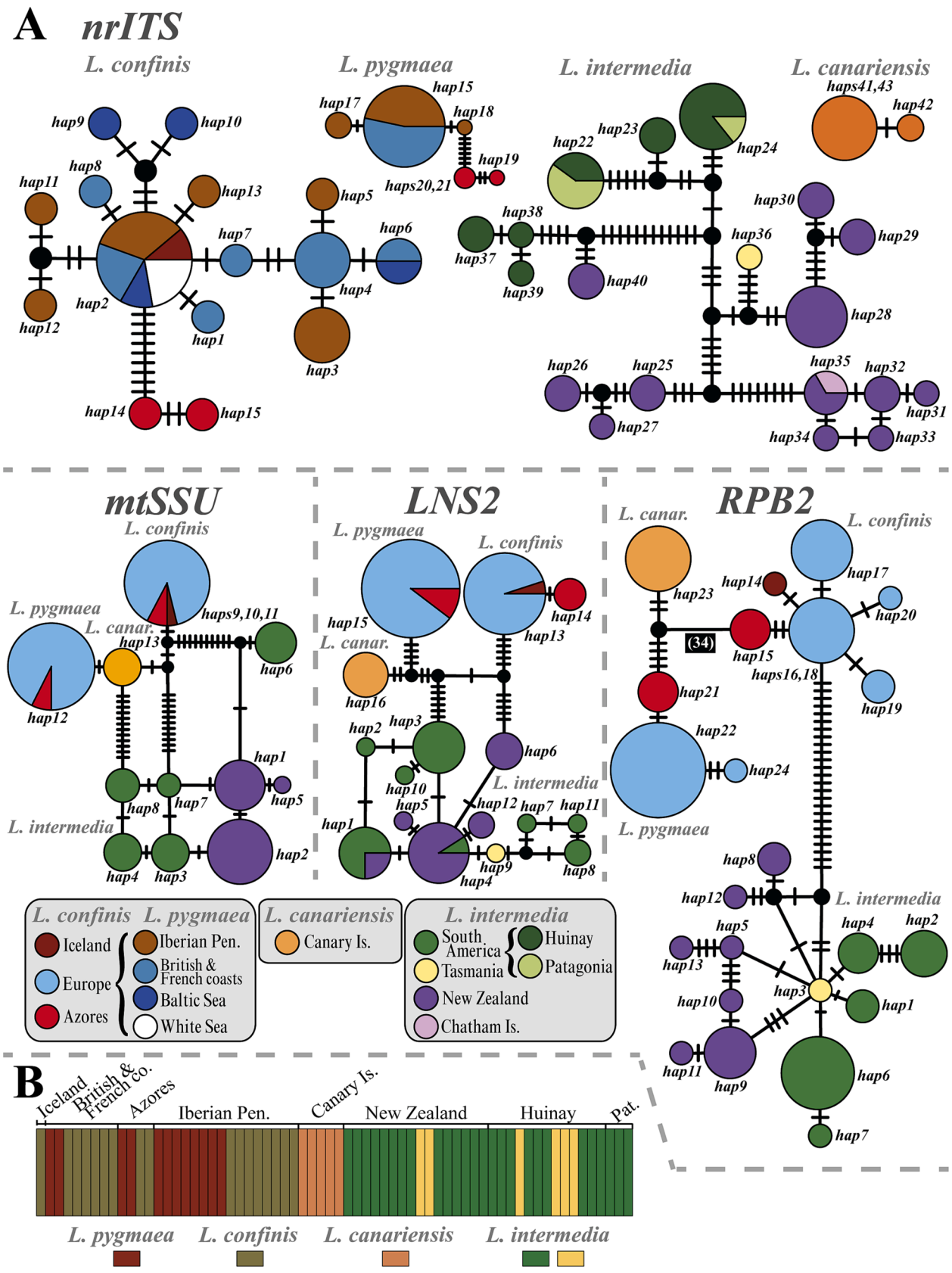

Fig. 2. Infraspecific genetic diversity of *Lichina* species. A. Statistical parsimony networks for haplotypes of four gene loci; colours indicate the localities where individuals were collected (see legend below); the sizes of circles in each network (but not among networks) are proportional to the numbers of individuals bearing the haplotype; circles may represent two or more haplotypes when these are separated only by indels; black-filled circles indicate missing haplotypes, and hatch marks indicate mutations. B. Admixture results ($K = 5$) from a Bayesian clustering analysis conducted with BAPS using SNP data from the four *Lichina* species.

Table 1
Marginal likelihood and Bayes factor values for the four alternative species delimitation models in *Lichina* and their motivation. The best model is highlighted in bold. Model 1 to 4 (M1-4) are also shown in Fig. 1B.

	Distinct species	Motivation	Path Sampling		Stepping-Stone	
			Ln (Marginal Likelihood)	2ln (Bayes Factor)	Ln (Marginal Likelihood)	2ln (Bayes Factor)
M1-Model 1 (four *Lichina* spp.)	New species *(L. canariensis)* / *L. pygmaea* / *L. confinis* / *L. intermedia*	Four partitions in the ABGD analysis of nrITS data; nrITS phylogeny; main phylogenetic clades in the four-locus topology	−7421.56	27.7	−7415.819	40.42
M2-Model 2 (five *Lichina* spp.)	New species *(L. canariensis)* / *L. pygmaea* / *L. confinis* / *L. intermedia* clade 1 / *L. intermedia* clade 2	Five partitions in the ABGD analysis of nrITS data; BAPS result	−7411.71	8	**−7395.6087**	**N/A**
M3-Model 3 (five *Lichina* spp.)	New species *(L. canariensis)* / *L. pygmaea* / *L. confinis* / *L. intermedia* (southern South America specimens) / *L. intermedia* (Tasmania + New Zealand + Chatham Isl. specimens)	According to geography and general morphology of thalli, the southern South America *L. intermedia* specimens are considered a different species	−7408.86	2.3	−7399.0617	6.906
M4-Model 4 (ten *Lichina* spp.)	New species *(L. canariensis)* / *L. pygmaea* / *L. confinis* / *L. intermedia* (seven clades within considered as different candidate species)	Five partitions in the ABGD analysis of nrITS data	**−7407.71**	**N/A**	−7406.4224	21.627

rocks, 2 February 2011, *A. de los Ríos* (MA-Lichen 24496 —holotype, TNF—isotype).

Etimology: The epithet refers to the Canary Islands archipelago where the new species has been found and from where it is so far only known.

Description: Thallus blackish, usually paler, light brown to olivaceous brown at the base, dwarf fruticose, forming patches up to 10 cm in size, branches from rounded to flattened (Fig. 3A), furcate, usually erect, although some thalli are prostrate, up to 0.75 mm long. Branches differ in thickness, with bases and apices narrower than middle branch, up to 700 × 250 μm in flattened branches and up to 500 μm in diam in rounded branches. Cortex distinct, hyaline, composed of densely packed shortly elongated cells, arranged in parallel to cortex surface, not longitudinally, up to 25 μm thick, may be absent or very reduced in some parts of the branch and at branch tips; photobiont layer 40–70 μm thick (-150 μm) with photobiont chains extending from the medullar layer to the cortex more or less perpendicularly, usually sinuous, rarely straight, cyanobiont *Rivularia* (Ortiz-Álvarez et al. 2015); central hyphal strand up to 300 μm thick, compact, composed of hyphae mostly running parallel to the main axis of the branch, with peripheral hyphae introducing into the photobiont layer (Fig. 3). Apothecia terminal to subterminal, (sub)globose, up to 500 μm in diameter; poriform, disc reddish to yellowish brown, rarely opened, frequently empty, thalline margin persisting, up to 135 μm thick; exciple distinct, hyaline, up to 60 μm thick, paraplectenchymatous, composed of small compressed rectangular cells; hymenium up to 375 μm high, KOH/IKI + weakly bluish green; paraphyses slender, septate, rarely branched, frequently anastomosed, with not widened tips. Asci prototunicate, narrowly clavate, up to 115 μm long, 8-spored, wall thin, non-amyloid, with no apical structures observed; ascospores hyaline, simple, broad ellipsoid, (21–)24–*25.62*–28(–33) × (9–)10–*12.03*–14(–15) μm (n = 30), wall thick in mature ascospores, up to 2 μm. Pycnidia terminal, (sub)globose, frequently flattened at the top, ostiole dark to pale frown, up to 25 μm thick, with several chambers in mature specimens; conidiophores simple, 25–30 × 1.5–3 μm; conidiospores hyaline, oblong to bacilliform, often with a flattened end, 3–*4*–5 × 1.5–*1.62*–2 μm (n = 37).

Habitat and distribution: The new species grows on rocks in the upper intertidal zone associated with barnacles, crustose red algae and free-living *Rivularia* colonies. So far, it is only known from three localities in Lanzarote, Gran Canaria and Tenerife (Canary Islands, Spain). The new taxon has been searched unsuccessfully in the other islands of the archipelago, and in the Madeira archipelago. According to current knowledge, *L. canariensis* does not appear to be a locally abundant species as is the case with the other two known North Atlantic species.

Notes: Lichina canariensis clearly resembles *L. pygmaea,* the taxon with which it had been confused up to now and which also occurs in the intertidal zone in the northern Atlantic. At first glance, *L. canariensis* may be considered a poorly developed morphotype of the latter. *Lichina pygmaea* thalli often reach 1 cm in height (Jørgensen 2007; Fletcher and Purvis 2009) compared to the maximum 0.75 cm measured for *L. canariensis,* although they are usually c. 0.5 cm. *Lichina pygmaea* branches are always flattened (to 2 mm, Fletcher and Purvis 2009) whereas *L. canariensis* may show flattened branches in prostrate thalli (to 0.7 mm) to more or less cylindrical branches in erect thalli (to 0.5 mm). *Lichina pygmaea* never shows cylindrical branches. In addition, *Lichina canariensis* never shows the typical palmate branching pattern found in *L. pygmaea*, the branches being furcate but not palmate. Anatomically, cortical layer in *L. pygmaea* is composed of more or less isodiametric cells (Schultz 2017, Fig. 4C), however in *L. canariensis*, the cortical layer is composed of shortly elongated to prismatic cells, orientated parallel to thallus surface, similar to a ring in transverse sections. Finally, *Lichina pygmaea* also shows larger apothecia (to 2 mm in diam) than *L. canariensis* (to 0.5 mm in diam). *Lichina confinis* is easily differentiated from *L. canariensis* by its thallus forming densely interwoven tufts of cylindrical coralloid branches and the smaller ovate ascopores 15–20 × 10–15 μm (Jørgensen 2007); in addition, *Lichina confinis* occurs in the supralittoral zone. *Lichina pygmaea* has been recorded from Tenerife and Gran Canaria, and *L. confinis* from Tenerife, Fuerteventura and Lanzarote (Arechavaleta et al. 2010). Old records should be revised and material compared with the description of *L. canariensis*. The Southern Hemisphere taxon *Lichina intermedia* shows a similar plasticity in branch morphology as *L. canariensis*, with more flattened branches in prostrate thalli and more cylindrical in erect ones (Schultz 2017). Branches are slightly thinner in *L. intermedia* (to 0.38 mm) compared to *L. canariensis* (to 0.7 mm). In addition, ascospores are slightly shorter in *L. intermedia* [(15–)17.8–*21.4*–25(–28.5) × (7–)9.0–*11.1*–13.2(–15) μm] than in *L. canariensis* [(21–)24–*25.62*–28(–33) × (9–)10–*12.03*–14(–15) μm].

Lichina is known to dwell highly diverse and distinct bacterial communities (West et al. 2018). In addition, *L. canariensis* often shows a thick biofilm layer on the cortex (Fig. 3D), including a rich morphological variety of cyanobacteria.

Other material studied: Lichina canariensis. Spain, Las Palmas, Gran Canaria, Las Palmas de Gran Canaria, intertidal zone in Playa de las Canteras, 28°8′55″N, 15°25′59.5″W, 0 m asl, on volcanic rocks, 2

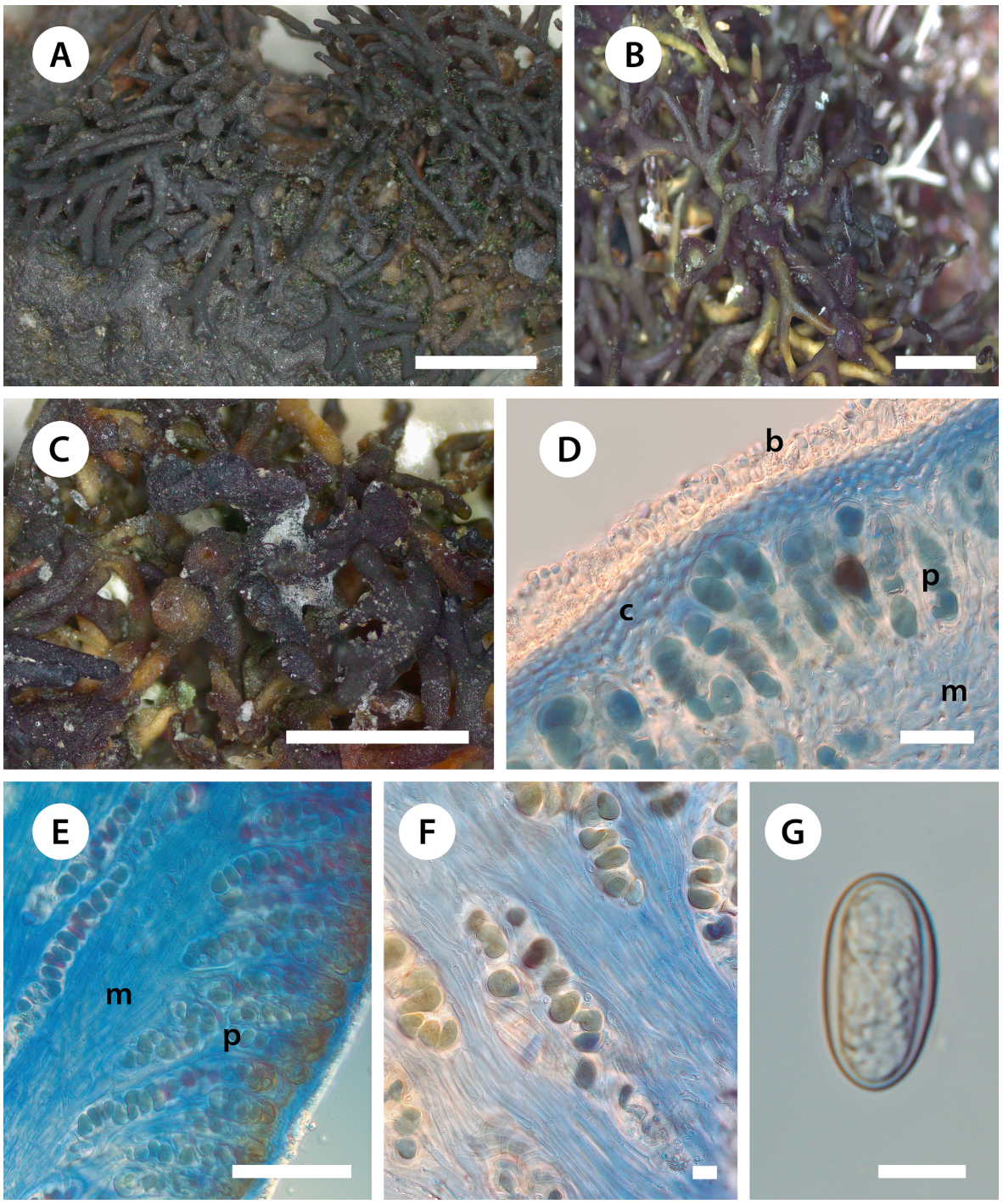

Fig. 3. A. Prostrate thallus with flattened and furcate branches (MA-Lichen 24498); B. Erect thallus with cylindrical branches (MA-Lichen 24490); C. Detail of apothecia (MA-Lichen 24498); D. Transverse section of a branch showing the cortex (c), medulla (m) and the photobiont layer (p) and the biofilm covering the thallus (b) (MA-Lichen 24490); E. Longitudinal section of a branch tip showing the photobiont layer (p) and the densely packed medullar hyphae (m) running in parallel to branch axis (MA-Lichen 24494); F. Detail of the medullar hyphae in longitudinal section and the *Rivularia* photobionts (MA-Lichen 24490); G. Ascospore (MA-Lichen 24494). Scales: A, B & C = 2 mm; D & F = 20 μm; E = 50 μm; G = 10 μm. D, E, F = Lactophenol blue; G = Water; D, E, F & G = Differential interference contrast (DIC). (For interpretation of the references to colour in this figure legend, the reader is referred to the web version of this article.)

February 2011, *A. de los Ríos* (MA-Lichen 24497; 24498); Las Palmas, Lanzarote, Arrieta, intertidal zone in Playa de Arrieta, 29°7′34.5″N; 13°27′53.8″W, 0 m asl, on volcanic rocks, 16 June 2011, *A. de los Ríos*, (MA-Lichen 24490, 24491, 24992, 24993, 24994, 24995; TNF); Santa Cruz de Tenerife, Puerto de la Cruz, intertidal zone in Playa de San Telmo, 28°25′3″N; 16°32′49″W, 0 m asl, on volcanic rocks, *R. Ortiz-Álvarez* (MA-Lichen 24499).

Lichina pygmaea. Spain, Asturias, Gozón. Playa del Bañugues, intertidal zone in Playa de Bañugues, 43°37′45″N, 5°50′39″W, 0 m asl, on limestone rocks, 26 May 2010, *S. Pérez-Ortega 2735, A. de los Ríos & M. Torralba* (MA-Lichen 19318); Spain, Asturias, Cudillero, intertidal zone in Playa del Silencio, 43°33′59″N, 6°17′13″W, 0 m asl, on acid rocks, 26 May 2010, *S. Pérez-Ortega 2731, A. de los Ríos & M. Torralba* (MA-Lichen 19316); Spain, Guipúzcoa, Hondarribia, intertidal zone close o Faro de

Híguer 43°23′35″N, 1°47′26″W, 0 m asl, on sandstone, 19 June 2009, *S. Pérez-Ortega 3065–1 & A. de los Ríos* (MA-Lichen 19339); Spain, Galicia, Pontevedra, Aguete, intertidal zone in Playa de Aguete, 42°22′26″N, 8°43′55″W, 0 m asl, on granitic rocks, 18 August 2008, *S. Pérez-Ortega 3057, S. Framil & N. Fernández* (MA-Lichen 19342).

Lichina intermedia. New Zealand, Northland, Waiheke, rocky seashore by Oakura Bay, 36°48′43.80″S, 175°02̀13.19″E, 0 m asl, on acid rocks, 13 November 2015, *A. de los Ríos* (MA-Lichen); New Zealand, Southland, rocky seashore by Kuri Bush, 46°01̀29.83″S, 170°13̀51.06″E, 0 m asl, on acid rocks, 26 November 2015, *A. de los Ríos & A. Knight* (MA-Lichen); New Zealand, Northland, rocky seashore by Matiatia Bay, 36°46′59″S, 174°59′24″E, 0 m asl, on acid rocks, 22 February 2015, *A. de los Ríos & D. Blanchon* (MA-Lichen); New Zealand, Southland, Akaroa, rocky seashore by Banks Peninsula, 43°48,835′S, 172°52,278′E, 0 m asl, on acid rocks, 16 November 2009, *A. de los Ríos* (MA-Lichen); Chile, Región de Magallanes y la Antártida Chilena, Tierra del Fuego, Isla Basket, 54°42′13″S, 71°34′53″W, 0 m asl, on acid rocks, 17 December 2009, *S. Pérez-Ortega* (MA-Lichen); Chile, Región de Magallanes y la Antártida Chilena, Isla Grande de Tierra del Fuego, Seno del Almirantazgo, Canal de Gabriel, 54°25′55″S, 70°7′ 48″W, 0 m asl, on basaltic rocks, 12 December 2009, S. Pérez-Ortega (MA-Lichen).

Lichina confinis. Spain, Asturias, Otur, supralittoral zone in playa de Otur, 43°33′16″N, 6° 35′62″W, 2 m asl, on limestone, 27 May 2010, *S. Pérez-Ortega 3059–3 & A. de los Ríos,* (MA-Lichen 19326); United Kingdom, Wales, Pembrokeshire, supralittoral zone at St. Brides Bay, 51°45′18.56″N, 5°11′17.42″W, 2 m asl, on argillite, 26 March 2011, *S. Pérez-Ortega 3152–2 & A. Orange* (MA-Lichen 19342); Spain, Pontevedra, Cangas, Cabo Home, supralittoral zone in Península del Mar, 42°15′5″N; 8°52′5″W, 2 m asl, on schists, 29 April 2011, *S. Pérez-Ortega 3135–2, A. de los Ríos, J. Pintado & M. Torralba* (MA-Lichen 19341); Portugal, Minho-Lima, Viana do Castelo, supralittoral zone in playa de Carreço, 41° 44′ 23″ N; 8° 52′W, 2 m asl, 30 April 2011, *S. Pérez-Ortega 3141, A. de los Ríos & M. Torralba* (MA-Lichen 19348).

3.4. Relationships between haplotypes

For convenience, haplotype networks of the more variable nrITS were generated independently for each species, whereas networks for the mtSSU, RPB2, and *LNS2* showed the most possible connections among the four species (Fig. 2A). In the Northern Hemisphere, *Lichina confinis* showed more nrITS haplotypes than *L. pygmaea*. The network of the former species had a star-like shape, with a central, more abundant haplotype that is widespread across the Atlantic coasts of Europe, from the Iberian Peninsula to Scandinavia and Iceland; stemming from this central haplotype, minor haplotypes were geographically restricted mainly to the Iberian Peninsula and the British and French coasts. In both *L. confinis* and *L. pygmaea*, two haplotypes were found in the Azores archipelago that differed from the mainland haplotypes by a considerable number of mutations. *Lichina canariensis* showed two haplotypes separated by just one mutation.

A star-like network was not found in the Southern Hemisphere *Lichina intermedia* based on nrITS data. Instead, two subnetwork areas containing haplotypes from southern South America and New Zealand were revealed; their connection and the connection of haplotypes within each subnetwork were generally made by a relatively high number of mutations. The New Zealand haplotype *hap40* was more closely related to Huinay haplotypes *hap37-39* than to other New Zealand haplotypes. No haplotypes were restricted to Patagonia; the Chatham Island *hap35* also occurred in New Zealand, whereas the Tasmanian *hap36* was isolated and closer to some New Zealand haplotypes (e.g., *hap28-30*).

Regarding the mtSSU, RPB2 and *LNS2* haplotype networks, several noticeable observations could be made. First, the reticulate structure of mtSSU and *LNS2* networks aligns with the lower phylogenetic resolution of these markers compared with the nrITS and RPB2 markers. For example, there is no unique path connecting the Southern Hemisphere *L. intermedia* to any Northern Hemisphere species. In contrast, the RPB2 network shows a clear connection of *L. intermedia* to *L. confinis*, although a high number of mutations separate these two species. Secondly, *L. canariensis* is always in closer proximity to *L. pygmaea* than to *L. confinis*. Thirdly, the Azorean haplotypes in *L. confinis* and *L. pygmaea* (mtSSU, *hap9-hap12*, respectively) and *L. pygmaea* (*LNS2*, *hap15*) also occurred in the European coasts; the Icelandic mtSSU *hap9* and *LNS2 hap13* of *L. confinis* were also shared in mainland Europe. Fourthly, the number of mutations separating southern South American and New Zealand mtSSU and *LNS2* haplotypes in *L. intermedia* is generally low (one); moreover, in the *LNS2* dataset, two haplotypes (*hap1*, *hap4*) are shared between these widely distant regions. Finally, in the RPB2 network, a central haplotype in *L. intermedia* was geographically restricted to Tasmania (*hap3*), and it was connected in a star-like manner to South American and New Zealand haplotypes, forming two independent network subareas.

3.5. Dating analyses

The primary and secondary calibration approaches conducted to infer a time frame for the speciation events in the genus *Lichina* generated different estimates (Fig. 4; Supplementary Table S5). Considering the four divergence events represented in the four-locus phylogeny (Fig. 1,4), the times to most recent ancestors (tmrca) inferred with the fossil calibration approach were lower and closer to present time than in the analyses using different nrITS substitution rates. The youngest median value for the crown of the genus *Lichina* (tmrca1) was estimated to be 22.8 Mya (early Miocene, primary calibration), while the oldest estimate was 84.65 Mya (Late Cretaceous, secondary calibration). The split between the Southern Hemisphere *L. intermedia* and the Northern Hemisphere *L. confinis* (tmrca2) was estimated to be as young as 14.56 Mya (middle Miocene), or as old as 57.3 Mya (late Paleocene). The divergence between *L. pygmaea* and the new species *L. canariensis* occurred 3.94 Mya or 15.19 Mya. Finally, diversification within *L. intermedia* started ca. 2.72 Mya (Pliocene) according to the primary calibration approach, or 13.61 Mya (middle Miocene) according to the alternative dating approach. The overlap in the estimated 95% highest posterior density intervals between the two calibration approaches (primary vs secondary) was absent in tmrca1, tmrca2 and tmrca4, and almost negligible in tmrca3.

As expected, the analysis using the faster-evolving substitution rate (*Melanohalea*) also generated younger time estimates compared to the slowest evolving rate of *Erysiphales*. Considering the crown of the genus *Lichina* (tmrca1) as an example, the date estimate inferred with the first approach was 62.29 Mya while the second approach dated this evolutionary event back to 84.65 Mya. Such date estimate discrepancies were much less pronounced on outer nodes of the phylochronogram (e.g., tmrca4) than in the inner tree nodes. The analyses conducted with the Gblocks-processed nrITS alignments, which were shorter in length due to the removal of ambiguously aligned fragments, tended to produce younger estimates than those obtained with the unprocessed datasets, especially at inner tree nodes (tmrca1 and tmrca2; Fig. 4). Thus, considering tmrca1 again, the analysis using the *Melanohalea* and *Erysiphales* substitution rates produced estimates of 53.55 and 72.02 Mya, respectively.

Lichina-specific nrITS substitution rates had a mean rate of 1.35×10^{-2} substitutions per site per million years, with a 95% highest posterior density interval ranging from 0.0043 to 0.0274 substitutions per site per million years (GBlocks-unprocessed nrITS alignment), or a mean rate of 1.18×10^{-2} substitutions per site per million years, with a 95% highest posterior density interval ranging from 0.0029 to 0.0242 substitutions per site per million years (GBlocks-processed nrITS alignment). Median values for the two estimates were 1.18×10^{-2} and 1.01×10^{-2} substitutions per site per million years, respectively.

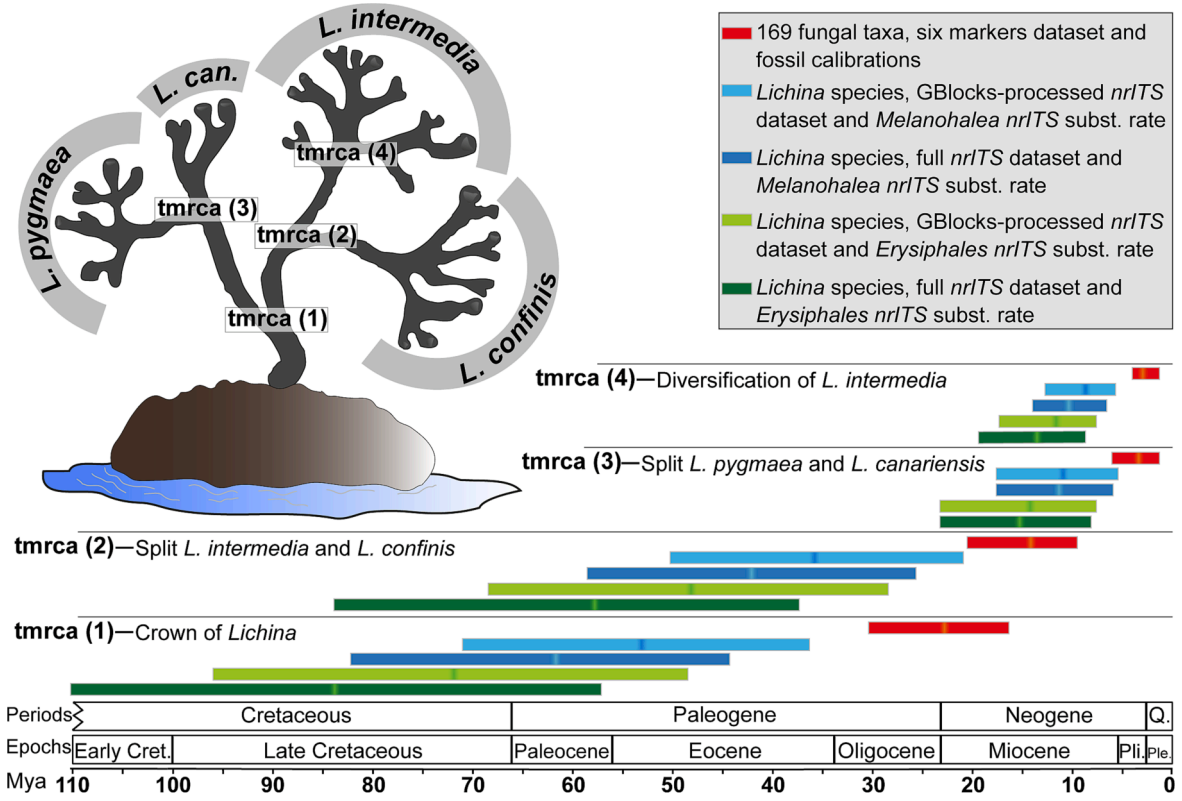

Fig. 4. The 95% highest posterior density intervals obtained in BEAST to frame the evolutionary history of the genus *Lichina*; four events represented by successive "tmrca" (time to the most recent ancestor) are shown; the lighter or darker mark in the each horizontal bar indicates de median value; age units are million years ago (Mya).

4. Discussion

The present phylogeographic study represents a necessary step for assessing species diversity in the lichenized fungal genus *Lichina* and for understanding their evolution through time and space. The number of taxa described under this genus, including infraspecific categories, is ca. 24–26, according to the fungal taxonomic databases MycoBank and Index Fungorum (searched 5 January 2022). However, Schultz (2017) indicated that non-maritime species that form pycnoascocarps (Henssen 1969) are phylogenetically placed outside the genus. In addition to *Lichina willeyi* (Tuck.) Henssen, outlier species probably include *L. tasmanica*, *L. rosulans*, *L. minutissima*, and *L. polycarpa*, all of them described by Henssen (1969, 1973). Other taxa formerly included in the genus but that might lay outside due to their characteristics are *L. antarctica* Crombie (Schultz 2017), reported from the Kerguelen Islands; *L. macrospora* Henssen, Büdel & Wessels, a species found along the edges of rivulets and streams at c. 1400 m above sea level in South Africa (Henssen et al. 1985); and *L. microcarpa*, a dubious species described by Montagne (1851) based on a collection from the Cayenne region in the French Guiana. As mentioned above, the majority of these species are non-maritime and are distributed in the Southern Hemisphere. The genus *Lichina* may be consequently reduced to the four maritime species studied in the present work, especially if varieties, forms and already synonymized taxa are accounted for (Schultz 2014; Index Fungorum; MycoBank). However, doubtful species must be assessed phylogenetically using a similar framework to the one developed here, which has proven useful to formally describe *L. canariensis* from the rocky seashores in the Canary Islands. Finally, "*Lichina sphaerospora* ad int.", from Livingston Island in Antarctica, may represent the fifth maritime species of this genus (Schultz 2017), although such hypothesis should be evaluated phylogenetically given the wide distribution of *L. intermedia* at high latitudes in the Southern Hemisphere. Indeed, a migratory pathway across the Sea of Hoces (Drake Passage) is reasonable, as inferred for other lichens (Fernández-Mendoza and Printzen 2013; Garrido-Benavent et al. 2018, 2021; Lagostina et al. 2021), and mosses (Biersma et al. 2017; Saługa et al. 2018).

The Northern Hemisphere *Lichina pygmaea*, *L. confinis*, and *L. canariensis* were well delineated as single, independent species across the different analytical approaches conducted in the present work. On the other hand, *Lichina intermedia* was segregated into varying numbers of species-level lineages depending on the implemented method: two (ABGD) or seven (bPTP). The segregation of specimens from Australasia into one candidate species, and those from South America into another, as would have been expected given the high geographic distance separating these two regions, did not receive much support. These results probably stem from the fact that *L. intermedia* hosts a much higher genetic diversity compared to the other three species, demonstrated by the comparatively high number of phylogenetic subclades displayed in single- and multi-locus phylograms. Therefore, ABGD, bPTP and the multispecies coalescent method (BFD) implemented to estimate and validate species boundaries are likely delimiting structure in *L. intermedia*, not species-level lineages (Sukumaran and Knowles 2017; Lücking et al. 2021). In consequence, the delimitation of species in *Lichina* seems more reasonable on the basis of supported phylogenetic clades, at least given the generated molecular dataset. This is also the most conservative option, as all studied populations of maritime *Lichina* in the Southern Hemisphere are kept under a single taxonomic entity. Furthermore, the nrITS seems a valuable species-level diagnostic marker for this genus, as proven for many other fungi (Schoch et al. 2012). The higher genetic diversity recovered in *L. intermedia* contrasts with the much lower genetic diversity found in all three taxa from the Northern Hemisphere. This fact may have resulted from the contrasting patterns in Pleistocene glaciations in the biota of the Northern and Southern

Hemispheres (Fraser et al. 2012, 2013).

The inferred phylogenies suggest that geographic isolation at the scale of million years played a pivotal role in the diversification of the genus. The different dating analyses estimated the start of that diversification to be 22.8 or 84.65 Mya. In the Northern Hemisphere, the lineage that represents *L. canariensis* likely split from an ancestor shared with *L. pygmaea* after a colonization of the Canary Islands. Migration could have taken place from any rocky seashore in mainland Europe, assuming that the past geographic distribution of *L. pygmaea* was similar to the present, or even from the Moroccan coast, where records of "*L. pygmaea*" are rare (Renaut et al. 1975). This event would have occurred between 3.94 Mya and 15.19 Mya (Miocene-Pliocene), coinciding with the volcanic origin of the oldest Canary Islands, between 11.6 and 15.5 Mya (Coello et al. 1992), precisely where *L. canariensis* has been collected so far (Tenerife, Gran Canaria and Lanzarote). Therefore, the similar or even younger origin of *L. canariensis* than the oldest Canary Island supports a past transatlantic dispersal event, and a subsequent colonization of various islands. Similarly, the origin of neo-endemic lichen species, such as in the genus *Nephroma,* was inferred to occur after the rise of the oldest Macaronesian islands (Sérusiaux et al. 2011), and additional evidences are found in invertebrates and plants (Juan et al. 2000; Cox et al. 2010; García-Verdugo et al. 2019).

An identical transatlantic crossing may describe the establishment of populations of *Lichina pygmaea* and *L. confinis* in the Azorean archipelago, which is ca. 1400 km off the Portuguese coasts. The younger age of these islands (Santa Maria, the oldest one, is ca. 8.2 Mya; França et al. 2003) compared with the Canary Islands may explain why genetic differentiation of island and mainland populations of these two species is much lower than the observed between *L. canariensis* and *L. pygmaea*. Indeed, incomplete allele sorting can be observed, as haplotypes of the more slowly evolving markers mtSSU and *LNS2* are still shared between Azorean and European populations. Transoceanic dispersal followed by genetic differentiation (and speciation) has been similarly documented for the endemic Azorean liverwort *Leptoscyphus azoricus* Grolle (Vanderpoorten and Long 2006). As for the Icelandic *L. confinis*, the sharing of identical haplotypes with several populations in the European coasts adds support to previous evidence indicating lichen migratory pathways across the northern Atlantic (Onuț-Brännström et al. 2018). Land in this volcanic island emerged at least 15 Mya (Foulger 2002; Denk et al. 2011) and the distance from other landmasses where *Lichina* species have been recorded, such as the British Isles, Scandinavia, or even the Faroe Islands, is around or less than 1000 km. Given the role of transatlantic migration events in shaping the evolution of this lichen genus in the Northern Hemisphere and the current distribution of extant species, it is still puzzling the extremely rare reports of *Lichina* in the eastern coasts of North America, as noted by Schultz (2017). A phylogenetic evaluation of the few collections (GBIF Secretariat, 2021) would be crucial to unveil the most likely colonization pathways across the Atlantic Ocean and compare them with the main wind or air currents, or even the routes of migratory birds (Gillespie et al. 2012; Fajardo et al. 2019).

The presence and dominance of *Lichina intermedia* across the Pacific Ocean has evolutionary and biogeographical relevance. Traditionally, two competing hypotheses have been invoked to explain widely disjunct distributions in lichens: dispersal or vicariance due to continental drift (e.g., Galloway 1988; Galloway & Aptroot 1995; Bjerke and Elvebakk 2004). Divergence times in dated molecular phylogenies are often used to test both hypotheses, assuming that a vicariant origin would be supported if time estimates for the separation of disjunct lineages predate or at least coincide with the breakup of Pangaea and Gondwana (mid-Jurassic to Late Cretaceous, ca. 174–66 Mya; Scotese 2001). However, the assessment of amphitropical distributions in lichens has frequently revealed long-distance dispersal in relatively recent times as the most likely origin for such disjunctions (Garrido-Benavent et al. 2018, 2021). On this basis, the sister relationship of *L. intermedia* with the Northern Hemisphere *L. confinis* was dated back to 14.56 or 57.3 Mya (primary and secondary calibration approaches, respectively), when the main continental landmasses were situated roughly at the same position as the present (Scotese 2001). Therefore, a shared ancestor between the two *Lichina* species had to disperse through the tropics, either in a single event, or following a stepping-stones mode (Fernández-Mendoza and Printzen 2013). The data available so far do not allow to decide in favor of one hypothesis or the other. Besides, long-distance dispersal may be again invoked to describe the origin of disjunct populations of *L. intermedia* in Southern Hemisphere landmasses. This distribution was established in the last 2.72 to 13.61 million years when landmasses at high latitudes in the Southern Hemisphere were already separated (Scotese 2001). Single- and four-locus phylograms, as well as haplotype networks and BAPS results, showed that populations on both sides are not genetically well distinguishable. The crossing of the Pacific by *L. intermedia* may have in fact occurred more than once, as suggested by the supported subclade in the nrITS tree hosting a few Chilean and New Zealand specimens, and also by the BAPS genetic assignment, which revealed two clusters shared between both regions. Widhelm et al. (2021) have recently revealed a similar distribution pattern of infraspecific genetic diversity among Australian, New Zealand and Chilean populations of the lichen *Pseudocyphellaria glabra* (Hook. F. & Taylor) C.W. Dodge, and explained it by frequent long-distance dispersal across the Pacific. This is also the explanation given for understanding the circumantarctic distribution of other spore-bearing organisms, like non-lichenized fungi (Moncalvo et al. 2008), mosses (Biersma et al. 2017) or ferns (Chao et al. 2014), as well as algae (Fraser et al. 2013) and streptophytes (Sanmartín and Ronquist 2004). Dispersal of *Lichina* through propagules (fungal ascospores and/or thallus fragments) across either the Southern or Northern Hemisphere could have been facilitated by water or wind currents (Golan and Pringle 2017; Fajardo et al. 2019), or even birds like albatrosses or shearwaters (Gillespie et al. 2012; Widhelm et al., 2021), which frequently visit the rocky seashores where *Lichina* species occur. Further evidence is needed to support any of those means of dispersal.

The time frames that served to discuss the most relevant events in the evolutionary history of the genus *Lichina* were estimated using either primary or secondary calibrations. Because secondary calibrations were based on the use of different nrITS substitution rates from lineages belonging to other fungal classes (*Eurotiomycetes* and *Lecanoromycetes*), results derived from the primary calibration, which is based on fossil data and a more extensive molecular marker and specimen datasets, are expected to be more accurate (Schenk 2016). For example, the diversification of the genus was estimated to be 22.8 or 84.65 Mya. Only the lower value, which was obtained using the primary calibration approach, agrees partially with the highest posterior density interval of 5 to 25 Mya for the *Lichina confinis-pygmaea* divergence obtained by Ortiz-Álvarez et al. (2015). Therefore, the present study demonstrates the effect of using one dating strategy or the other, although, in the particular case of *Lichina*, the results of the two strategies are consistent as far as the interpretation of the evolution and biogeography of the genus is concerned. Finally, two *Lichina*-specific nrITS substitution rates (1.35×10^{-2} and 1.18×10^{-2} substitutions per site per million years) have been inferred based on the compiled molecular and species dataset. These are an order of magnitude faster than the rates of 2.52×10^{-3} substitutions per site per million years estimated for the non-lichenized *Erysiphales* (*Eurotiomycetes* Takamatsu and Matsuda 2004) and 3.41×10^{-3} substitutions per site per million years estimated for the lichenized genus *Melanohalea* (*Lecanoromycetes*, Leavitt et al. 2012). Differences in generation times among lineages might explain this variability, as discussed for discrepancies in nrITS substitution rates between herbaceous and woody plants (Kay et al. 2006). It is consequently expected that the newly generated rates are more appropriate to (and trigger) further dating studies in *Lichina* and related lineages in *Lichinomycetes*.

5. Conclusions

The comprehensive specimen dataset assembled in the present study, which covers most of the known worldwide distribution of the genus, has allowed the establishment of a sound framework for future research in the cyanolichen genus *Lichina*. The obtained data show that the current diversity and distribution of *Lichina* species and their populations in the two hemispheres resulted from a complex and long history of dispersals across great expanses of water and a subsequent evolution under varying regimes of geographic isolation. Further work could expand our knowledge of the genus, by corroborating if the non-maritime species of *Lichina* do indeed belong to another genus, and whether the Antarctic collections represent a new species or, alternatively, the southern-most population of *L. intermedia*. A genetic characterization of the cyanobacteria associated with *L. intermedia* species is also required, as it could shed light on the role of these photobionts in the process of colonization of the Southern Hemisphere and provide more information about the lichen ecological preferences.

CRediT authorship contribution statement

Isaac Garrido-Benavent: Writing – original draft, Conceptualization, Methodology, Formal analysis, Resources, Project administration. **Asunción de los Ríos:** Resources, Writing – review & editing. **Jano Núñez-Zapata:** Methodology, Writing – review & editing. **Rüdiger Ortiz-Álvarez:** Conceptualization, Resources, Writing – review & editing. **Matthias Schultz:** Conceptualization, Writing – review & editing. **Sergio Pérez-Ortega:** Conceptualization, Methodology, Resources, Project administration, Writing – review & editing, Funding acquisition.

Declaration of Competing Interest

The authors declare that they have no known competing financial interests or personal relationships that could have appeared to influence the work reported in this paper.

Acknowledgements

The authors thank Allison Knight (Otago, NZ), Mercedes Vivas (Pamplona, ES), Ulrik Søchting (Copenhagen, DK) for contributing to collections. We also thank María Prieto (Madrid, Spain) for her advice on the amplification of molecular markers in *Lichina*. SPO thanks Leopoldo G. Sancho and Esteban Manrique (Madrid, ES) for the opportunity to join the Tierra del Fuego (2009) and Huinay (2014) expeditions respectively.

Funding

Funding for this study was supported by the grant RYC-2014–16784. IG-B was partially supported by the Programa Operativo de Empleo Juvenil y la Iniciativa de Empleo Juvenil (YEI) de la Comunidad de Madrid (CAMD_MAD_RJB_001). SP-O was supported by a 'Ramón y Cajal' contract (RYC-2014–16784) from the Spanish Ministry of Science, Innovation and Universities. AdR was supported by CTM2015-64728-C2-2-R (MINECO/FEDER, UE), and partly by grant CTM2017-84441-R.

Appendix A. Supplementary material

Supplementary data to this article can be found online at https://doi.org/10.1016/j.ympev.2023.107829.

References

Arechavaleta, M., Rodríguez, S., Zurita, N., García A. 2010. Lista de especies silvestres de Canarias. Hongos, plantas y animales terrestres. Gobierno de Canarias.

Biersma, E.M., Jackson, J.A., Hyvönen, J., Koskinen, S., Linse, K., Griffiths, H., Convey, P., 2017. Global biogeographic patterns in bipolar moss species. Roy. Soc. Open Sci. 4, 170147.

Bjerke, J.W., Elvebakk, A., 2004. Distribution of the lichen genus *Flavocetraria (Parmeliaceae, Ascomycota)* in the Southern Hemisphere. New Zeal. J. Bot. 42, 647–656.

Brodo, I.M., Santesson, R., 1997. Lichens of the queen charlotte islands, british columbia, canada. 3. Marine species of *Verrucaria (Verrucariaceae, Ascomycotina)*. J. Hattori Bot. Lab. 82, 27–37.

Castresana, J., 2000. Selection of conserved blocks from multiple alignments for their use in phylogenetic analysis. Mol. Biol. Evol. 17, 540–552.

Chao, Y.S., Rouhan, G., Amoroso, V.B., Chiou, W.L., 2014. Molecular phylogeny and biogeography of the fern genus *Pteris (Pteridaceae)*. Ann Bot.-London 114, 109–124.

Chappuis, E., Terradas, M., Cefalì, M.E., Mariani, S., Ballesteros, E., 2014. Vertical zonation is the main distribution pattern of littoral assemblages on rocky shores at a regional scale. Estuar. Coast. Shelf. Sci. 147, 113–122.

Chrismas, N.A., Allen, R., Hollingsworth, A.L., Taylor, J.D., Cunliffe, M., 2021. Complex photobiont diversity in the marine lichen *Lichina pygmaea*. J. Mar. Biological Asso. UK 101, 667–674.

Coello, J., Cantagrel, J.M., Hernán, F., Fúster, J.M., Ibarrola, E., Ancochea, E., Casquet, C., Jamond, C., Díaz de Téran, J.-R., Cendrero, A., 1992. Evolution of the eastern volcanic ridge of the Canary Islands based on new K-Ar data. J. Volcanol. Geoth. Res. 53, 251–274.

Corander, J., Marttinen, P., 2006. Bayesian identification of admixture events using multilocus molecular markers. Mol. Ecol. 15, 2833–2843.

Corander, J., Marttinen, P., Sirén, J., Tang, J., 2008. Enhanced Bayesian modelling in BAPS software for learning genetic structures of populations. BMC Bioinf. 9, 1–14.

Cox, S.C., Carranza, S., Brown, R.P., 2010. Divergence times and colonization of the Canary Islands by *Gallotia* lizards. Mol. Phylogenet. Evol. 56, 747–757.

Delmail, D., Grube, M., Parrot, D., Cook-Moreau, J., Boustie, J., Labrousse, P., Tomasi, S. 2013. Halotolerance in lichens: symbiotic coalition against salt stress. In: Ahmad, P., Azooz, M., Prasad, M. (Eds.), Ecophysiology and responses of plants under salt stress. Springer, New York, pp. 115–148).

Denk, T., Grímsson, F., Zetter, R., Símonarson, L.A., 2011. The biogeographic history of Iceland–the North Atlantic land bridge revisited. In: Late Cainozoic Floras of Iceland. Topics in Geobiology, Vol. 35. Springer, Dordrecht, pp. 647–668.

Drummond, A.J., Suchard, M.A., Xie, D., Rambaut, A., 2012. Bayesian phylogenetics with BEAUti and the BEAST 1.7. Mol. Biol. Evol 29, 1969–1973.

Fajardo, J., Mateo, R.G., Vargas, P., Fernández-Alonso, J.L., Gómez-Rubio, V., Felicísimo, Á.M., Muñoz, J., 2019. The role of abiotic mechanisms of long-distance dispersal in the American origin of the Galápagos flora. Global Ecol. Biogeogr. 28, 1610–1620.

Fernández-Mendoza, F., Printzen, C., 2013. Pleistocene expansion of the bipolar lichen *Cetraria aculeata* into the Southern Hemisphere. Mol. Ecol. 22, 1961–1983.

Fletcher, A., 1980. Marine and maritime lichens of rocky shores: their ecology, physiology and biological interactions. In: Price, J.H., Irvine, D.E.G., Farnham, W.F. (Eds.), The Shore Environment, Vol. 2. Academic Press, London, pp. 789–842.

Fletcher, A., Purvis, O.W., 2009. Lichina. In: Smith, C.W., Aptroot, A., Coppins, B.J., Fletcher, A., Gilbert, O.L., James, P.W., Wolseley, P.A. (Eds.), The Lichens of Great Britain and Ireland. British Lichen Society, London, pp. 556–557.

Flewelling, A.J., Currie, J., Gray, C.A., Johnson, J.A., 2015. Endophytes from marine macroalgae: promising sources of novel natural products. Curr. Sci. India 109, 88–111.

Foulger, G.R., 2002. Plumes, or plate tectonic processes? Astron. Geophys. 43, 6–19.

França, Z., Cruz, J.V., Nunes, J.C., Forjaz, V.H., 2003. Geologia dos Açores: uma perspectiva actual. Açoreana 10, 11–140.

Fraser, C.I., Nikula, R., Ruzzante, D.E., Waters, J.M., 2012. Poleward bound: biological impacts of Southern Hemisphere glaciation. Trends Ecol. Evol. 27, 462–471.

Fraser, C.I., Zuccarello, G.C., Spencer, H.G., Salvatore, L.C., Garcia, G.R., Waters, J.M., 2013. Genetic affinities between trans-oceanic populations of non-buoyant macroalgae in the high latitudes of the Southern Hemisphere. PLoS One 8, e69138.

Furbino, L.E., Pellizzari, F.M., Neto, P.C., Rosa, C.A., Rosa, L.H., 2018. Isolation of fungi associated with macroalgae from maritime Antarctica and their production of agarolytic and carrageenolytic activities. Pol. Biol. 41, 527–535.

Galloway, D.J., 1988. Plate tectonics and the distribution of cool temperate Southern Hemisphere macrolichens. Bot.l. J. Linn. Soc. 96, 45–55.

Galloway, D.J., Aptroot, A., 1995. Bipolar lichens: a review. Cryptogam. Bot. 5, 184–189.

García-Verdugo, C., Caujapé-Castells, J., Sanmartín, I., 2019. Colonization time on island settings: lessons from the Hawaiian and Canary Island floras. Bot. J. Linn. Soc. 191, 155–163.

Garrido-Benavent, I., de los Ríos, A., Fernández-Mendoza, F., Pérez-Ortega, S. 2018. No need for stepping stones: direct, joint dispersal of the lichen-forming fungus *Mastodia tessellata* (*Ascomycota*) and its photobiont explains their bipolar distribution. J. Biogeogr. 45, 213–224.

Garrido-Benavent, I., Pérez-Ortega, S., de los Ríos, A., Mayrhofer, H., Fernández-Mendoza, F. 2021. Neogene speciation and Pleistocene expansion of the genus *Pseudephebe* (*Parmeliaceae*, lichenized fungi) involving multiple colonizations of Antarctica. Mol. Phylogenet. Evol. 155, 107020.

GBIF Secretariat 2021. *Lichina* C.Agardh. GBIF Backbone Taxonomy. Checklist dataset. https://doi.org/10.15468/39omei (accessed 12 January 2022).

Gillespie, R.G., Baldwin, B.G., Waters, J.M., Fraser, C.I., Nikula, R., Roderick, G.K., 2012. Long-distance dispersal: a framework for hypothesis testing. Trends Ecol. Evol. 27, 47–56.

Godinho, V.M., Furbino, L.E., Santiago, I.F., Pellizzari, F.M., Yokoya, N.S., Pupo, D., Alves, T.M.A., Junior, P.A.S., Romanha, A.J., Zani, C.L., Cantrell, C.L., Rosa, C.A.,

Rosa, L.H., 2013. Diversity and bioprospecting of fungal communities associated with endemic and cold-adapted macroalgae in Antarctica. ISME J. 7, 1434–1451.
Golan, J.J., Pringle, A., 2017. Long-distance dispersal of fungi. Microbiol. Spectr. 5, 5.
Grummer, J.A., Bryson Jr, R.W., Reeder, T.W., 2014. Species delimitation using Bayes factors: simulations and application to the *Sceloporus scalaris* species group (*Squamata*: *Phrynosomatidae*). Syst. Biol. 63, 119–133.
Hawksworth, D.L., Grube, M., 2020. Lichens redefined as complex ecosystems. New Phytol. 227, 1281.
Heled, J., Drummond, A.J., 2010. Bayesian inference of species trees from multilocus data. Mol. Biol. Evol. 27, 570–580.
Henssen, A., 1969. Three non-marine species of the genus *Lichina*. Lichenologist 4, 88–98.
Henssen, A., 1973. New or interesting cyanophilic lichens I. Lichenologist 5, 444–451.
Henssen, A., Büdel, B., Wessels, D., 1985. New or interesting members of the *Lichinaceae* from southern Africa I. Species from northern and eastern Transvaal. Mycotaxon 22, 169–195.
Jørgensen, P.M. 2007. *Lichinaceae*. In: Ahti, T., Jørgensen, P.M., Kristinsson, H., Moberg, R., Søchting, U., Thor, G. (Eds.), Nordic Lichen Flora. Vol. 3: Cyanolichens. Nordic Lichen Society, Uppsala, pp: 46–76.
Juan, C., Emerson, B.C., Oromí, P., Hewitt, G.M. 2000. Colonization and diversification: towards a phylogeographic synthesis for the Canary Islands. Trends Ecol. Evol. 15, 104–109.
Kass, R.E., Raftery, A.E., 1995. Bayes factors. J. Am. Stat. Assoc. 90, 773–795.
Katoh, K., Standley, D.M., 2013. MAFFT multiple sequence alignment software version 7: improvements in performance and usability. Mol. Biol. Evol. 30, 772–780.
Kay, K.M., Whittall, J.B., Scott, A.H., 2006. A survey of nuclear ribosomal internal transcribed spacer substitution rates across angiosperms: an approximate molecular clock with life history effects. BMC Evol. Biol. 6, 36.
Kohlmeyer, J., Hawksworth, D.L., Volkmann-Kohlmeyer, B., 2004. Observations on two marine and maritime "borderline" lichens: *mastodia tessellata* and *Collemopsidium pelvetiae*. Mycol. Progr. 3, 51–56.
Kumar, S., Stecher, G., Li, M., Knyaz, C., Tamura, K., 2018. MEGA X: molecular evolutionary genetics analysis across computing platforms. Mol. Biol. Evol. 35, 1547.
Lagostina, E., Andreev, M., Dal Grande, F., Grewe, F., Lorenz, A., Lumbsch, H.T., Rozzi, R., Ruprecht, U., Sancho, L.G., Søchting, U., Scur, M., Wirtz, N., Printzen, C., 2021. Effects of dispersal strategy and migration history on genetic diversity and population structure of Antarctic lichens. J. Biogeogr. 48, 1635–1653.
Lamb, I.M., 1948. Antarctic pyrenocarp lichens. Discov. Rep. 25, 1–30.
Lanfear, R., Calcott, B., Ho, S.Y., Guindon, S., 2012. PartitionFinder: combined selection of partitioning schemes and substitution models for phylogenetic analyses. Mol. Biol. Evol. 29, 1695–1701.
Lartillot, N., Philippe, H., 2006. Computing Bayes factors using thermodynamic integration. Syst. Biol. 55, 195–207.
Leavitt, S.D., Esslinger, T.L., Divakar, P.K., Lumbsch, H.T., 2012. Miocene and Pliocene dominated diversification of the lichen-forming fungal genus *Melanohalea (Parmeliaceae*, *Ascomycota*) and Pleistocene population expansions. BMC Evol. Biol. 12, 176.
Leigh, J.W., Bryant, D., 2015. PopART: full-feature software for haplotype network construction. Methods Ecol. Evol. 6, 1110–1116.
Letunic, I., Bork, P., 2021. Interactive Tree Of Life (iTOL) v5: an online tool for phylogenetic tree display and annotation. Nucleic Acids Res. 49, W293–W296.
Librado, P., Rozas, J., 2009. DnaSP v5: a software for comprehensive analysis of DNA polymorphism data. Bioinformatics 25, 1451–1452.
Lücking, R., 2019. Stop the abuse of time! Strict temporal banding is not the future of rank-based classifications in fungi (including lichens) and other organisms. Crc. Cr. Rev. Plant Sci. 38, 199–253.
Lücking, R., Leavitt, S.D., Hawksworth, D.L., 2021. Species in lichen-forming fungi: balancing between conceptual and practical considerations, and between phenotype and phylogenomics. Fungal Divers. 109, 99–154.
Maddison, W.P., Maddison, D.R. 2014. Mesquite: A modular system for evolutionary analysis (Version 3.01). http://mesquiteproject.org.
Miller, M.A., Pfeiffer, W., Schwartz, T. 2010. Creating the CIPRES Science Gateway for inference of large phylogenetic trees. In: Proceedings of the Gateway Computing Environments Workshop (GCE). New Orleans, pp. 1–8.
Mitchell, J.K., Garrido-Benavent, I., Quijada, L., Pfister, D.H., 2021. *Sareomycetes*: more diverse than meets the eye. IMA Fungus 12, 1–36.
Moncalvo, J.-M., Buchanan, P.K., 2008. Molecular evidence for long distance dispersal across the Southern Hemisphere in the *Ganoderma applanatum-australe* species complex (*Basidiomycota*). Mycol. Res. 112, 425–436.
Montagne, J.P.F.C., 1851. Cryptogamia Guyanensis seu plantarum cellularium in Guyana gallica annis 1835–1849 a cl. Leprieur collectarum enumeratio universalis. Ann. Sci. Nat. Bot. 16, 47–81.
Onuț-Brännström, I., Benjamin, M., Scofield, D.G., Heiðmarsson, S., Andersson, M.G., Lindström, E.S., Johannesson, H., 2018. Sharing of photobionts in sympatric populations of *Thamnolia* and *Cetraria* lichens: evidence from high-throughput sequencing. Sci. Rep.-UK 8, 1–14.
Orange, A., 2012. Semi-cryptic marine species of *Hydropunctaria (Verrucariaceae*, lichenized *Ascomycota*) from north-west Europe. Lichenologist 44, 299–320.
Ortiz-Álvarez, R., de los Ríos, A., Fernández-Mendoza, F., Torralba-Burrial, A., Pérez-Ortega, S. 2015. Ecological specialization of two photobiont-specific maritime cyanolichen species of the genus *Lichina*. PLoS One 10, e0132718.
Pérez-Ortega, S., Garrido-Benavent, I., Grube, M., Olmo, R., de los Ríos, A., 2016. Hidden diversity of marine borderline lichens and a new order of fungi: *collemopsidiales (Dothideomyceta*). Fungal Divers. 80, 285–300.
Pérez-Ortega, S., Miller, K.A., de los Rios, A., 2018. Challenging the lichen concept: *Turgidosculum ulvae (Verrucariaceae*) represents an independent photobiont shift to a multicellular blade-like alga. Lichenologist 50, 341–356.
Puillandre, N., Lambert, A., Brouillet, S., Achaz, G.J.M.E., 2012. ABGD, automatic barcode gap discovery for primary species delimitation. Mol. Ecol. 21, 1864–1877.
Rambaut, A., Drummond, A.J., Xie, D., Baele, G., Suchard, M.A., 2018. Posterior summarization in Bayesian phylogenetics using Tracer 1.7. Syst. Biol. 67, 901.
Renaut, J., Sasson, A., Pearson, H.W., Stewart, W.D., 1975. Nitrogen-fixing algae in Morocco. In: Stewart, W.D.P. (Ed.), Nitrogen fixation by free-living microorganisms. Cambridge University Press, pp. 229–246.
Saługa, M., Ochyra, R., Żarnowiec, J., Ronikier, M., 2018. Do Antarctic populations represent local or widespread phylogenetic and ecological lineages? Complicated fate of bipolar moss concepts with *Drepanocladus longifolius* as a case study. Org. Divers. Evol. 18, 263–278.
Sanmartín, I., Ronquist, F., 2004. Southern Hemisphere biogeography inferred by event-based models: plant versus animal patterns. Syst. Biol. 53, 216–243.
Schenk, J.J., 2016. Consequences of secondary calibrations on divergence time estimates. PLoS One 11, e0148228.
Schoch, C.L., Seifert, K.A., Huhndorf, S., Robert, V., Spouge, J.L., Levesque, C.A., Che, W., et al., 2012. Nuclear ribosomal internal transcribed spacer (ITS) region as a universal DNA barcode marker for *Fungi*. P. Natl. Acad. Sci. USA 16, 6241–6246.
Schultz, M., 2014. Significant type collections of *Lichinaceae* and allied lichenized ascomycetes in the herbaria of the Natural History Museum, Vienna (W) and the Institute of Botany, Vienna University (WU). Ann. Nat. Hist. Mu. Wien Ser. B Bot. Zool. 116, 207–246.
Schultz, M., 2017. Morphological and molecular data support *Lichina intermedia* as a distinct austral-marine species in the *L. pygmaea* group. Lichenologist 49, 321–332.
Scotese, C.R., 2001. Atlas of Earth history. University of Texas, Arlington.
Sérusiaux, E., Villarreal A, J.C., Wheeler, T., Goffinet, B. 2011. Recent origin, active speciation and dispersal for the lichen genus *Nephroma* (*Peltigerales*) in Macaronesia. J. Biogeogr. 38, 1138–1151.
Stamatakis, A., 2006. RAxML-VI-HPC: maximum likelihood-based phylogenetic analyses with thousands of taxa and mixed models. Bioinformatics 22, 2688–2690.
Stamatakis, A., Hoover, P., Rougemont, J., 2008. A fast bootstrapping algorithm for the RAxML web-servers. Syst. Biol. 57, 758–771.
Stielow, J.B., Levesque, C.A., Seifert, K.A., Meyer, W., Iriny, L., Smits, D., Renfurm, R., Verkley, G.J.M., et al., 2015. One fungus, which genes? Development and assessment of universal primers for potential secondary fungal DNA barcodes. Persoonia 35, 242.
Sukumaran, J., Knowles, L.L., 2017. Multispecies coalescent delimits structure, not species. P. Natl. Acad. Sci. USA 114, 1607–1612.
Takamatsu, S., Matsuda, S., 2004. Estimation of molecular clocks for *ITS* and *28S* rDNA in *Erysiphales*. Mycoscience 45, 340–344.
Templeton, A.R., Crandall, K.A., Sing, C.F., 1992. A cladistic analysis of phenotypic associations with haplotypes inferred from restriction endonuclease mapping and DNA sequence data. III. Cladogram estimation. Genetics 132, 619–633.
Vanderpoorten, A., Long, D.G., 2006. Budding speciation and neotropical origin of the Azorean endemic liverwort, *Leptoscyphus azoricus*. Mol. Phylogenet. Evol. 40, 73–83.
West, N.J., Parrot, D., Fayet, C., Grube, M., Tomasi, S., Suzuki, M.T., 2018. Marine cyanolichens from different littoral zones are associated with distinct bacterial communities. PeerJ 6, e5208.
Widhelm, T.J., Grewe, F., Huang, J.P., Ramanauskas, K., Mason-Gamer, R., Lumbsch, H. T., 2021. Using RADseq to understand the circum-Antarctic distribution of a lichenized fungus, *Pseudocyphellaria glabra*. J. Biogeogr. 48, 78–90.
Xie, W., Lewis, P.O., Fan, Y., Kuo, L., Chen, M.H., 2011. Improving marginal likelihood estimation for Bayesian phylogenetic model selection. Syst. Biol. 60, 150–160.
Zhang, J., Kapli, P., Pavlidis, P., Stamatakis, A., 2013. A general species delimitation method with applications to phylogenetic placements. Bioinformatics 29, 2869–2876.